

---

# Membrane Nanotubes

I. Derényi<sup>1</sup>, G. Koster<sup>2,3</sup>, M.M. van Duijn<sup>4</sup>, A. Czövek<sup>1</sup>, and M. Dogterom<sup>3</sup>,  
and J. Prost<sup>2,5</sup>

<sup>1</sup> Department of Biological Physics, Eötvös University, Pázmány P. stny. 1A,  
H-1117 Budapest, Hungary  
[derenyi@angel.elte.hu](mailto:derenyi@angel.elte.hu)

<sup>2</sup> Institut Curie, UMR 168, 26 rue d'Ulm, 75248 Paris Cédex 05, France  
[gerbrand.koster@curie.fr](mailto:gerbrand.koster@curie.fr)

<sup>3</sup> FOM Institute for Atomic and Molecular Physics (AMOLF), Kruislaan 407,  
1098 SJ Amsterdam, The Netherlands  
[dogterom@amolf.nl](mailto:dogterom@amolf.nl)

<sup>4</sup> Department of Bioengineering, University of California Berkeley, Berkeley, CA  
94720-1762  
[vanduijn@berkeley.edu](mailto:vanduijn@berkeley.edu)

<sup>5</sup> ESPCI, 10 rue Vauquelin, 75231 Paris Cédex 05, France  
[jacques.prost@curie.fr](mailto:jacques.prost@curie.fr)

**Abstract.** There is a growing pool of evidence showing the biological importance of membrane nanotubes (with diameter of a few tens of nanometers and length upto tens of microns) in various intra- and intercellular transport processes. These ubiquitous structures are often formed from flat membranes by highly localized forces generated by either the pulling of motor proteins or the pushing of polymerizing cytoskeletal filaments. In this chapter we give an overview of the theory of membrane nanotubes, their biological relevance, and the most recent experiments designed for the study of their formation and dynamics. We also discuss the effect of membrane proteins or lipid composition on the shape of the tubes, and the effect of antagonistic motor proteins on tube formation.

## 7.1 Introduction

Eukaryotic cells are typically a few microns to a few tens of microns in size. Even at these small scales, there is a clear organization of spatially and functionally separated compartments (organelles) for different cellular functions: the nucleus for coding and storing the genetic information, the endoplasmic reticulum (ER) for the synthesis of proteins and lipids, the Golgi apparatus for the sorting of proteins according to their destination, the mitochondria for ATP production, or the chloroplasts for photosynthesis. A much-simplified sketch of a eukaryotic cell is presented in Fig. 7.1. The cells, and the organelles within them, are bounded and separated from the rest of the world

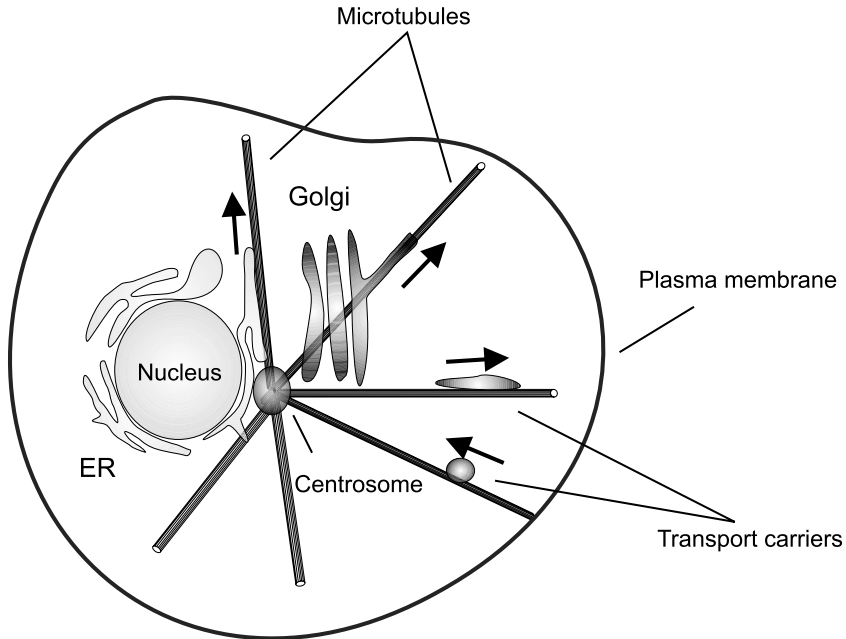


**Fig. 7.1.** Sketch of the internal organization of a eukaryotic cell. The *arrows* indicate the movement of membrane compartments along the microtubule cytoskeleton

by membranes. These membranes are made up of a mixture of different types of lipids that form a bilayer, and also contain a large number of membrane proteins.

### 7.1.1 In vivo Occurrences of Membrane Tubes

One important mechanism through which different compartments are shaped and spatially distributed is the action of motor proteins and the cytoskeleton. The cytoskeleton forms a dense network of tracks throughout the cell, and functions as an infrastructure for the movement of motor proteins that pull on the membrane compartments. This results either in the movement of the compartments through the cell or, if opposing forces are present, in their deformation, such as the formation and elongation of membrane tubes (also known as tethers), which are only a few tens of nanometers in diameter, but can reach tens of microns in length.

Motor proteins convert the chemical energy of ATP or GTP into mechanical work, and can typically generate forces up to 6 pN (the stall force [1]). Based on sequence homology, there are three main families of motors: kinesins, dyneins, and myosins [2]. Kinesin and dynein move along microtubules (MTs), whereas myosin along actin filaments. MTs grow by the polymerization of 8-nm-long tubulin dimers, which gives them a natural periodic and asymmetric

structure. Motors recognize this asymmetry: kinesin moves towards the plus-end, while dyneins move towards the minus-end of the MT in 8-nm steps [3]. There are, however, exceptions: the kinesin-family protein *ncd* [4] moves in the minus-end direction. While the details of the movement of individual motors begin to be unraveled [2, 5–8], it is clear that dimerization (or oligomerization) of motor proteins is crucial to their processivity (i.e., the number of steps taken before dissociation from the MT).

Conventional kinesin e.g., which is a dimer, takes on average  $\sim 100$  steps of 8 nm, and it can move at speeds up to  $1 \mu\text{m/s}$  [2]. When an external force is applied to kinesin (e.g., with optical tweezers or through cargo), the speed of the motor decreases until it stops moving at the stall force and, at the same time, the average number of steps before detachment decreases. Dynein, the dominant motor for minus-end directed movement along MTs, consists of a complex of proteins [9], making it difficult to work with for in vitro studies (genetic modification, expression, and purification). *Ncd* has been shown to be a non-processive motor: upon each contact with a MT it moves  $\sim 9$  nm and subsequently detaches [10]. The speed at which *ncd* can move MTs in gliding assay [2] has been measured to be  $0.1\text{--}0.15 \mu\text{m/s}$  [11].

The different organelles in cells have characteristic shapes, which are dynamic in the sense that they are constantly being remodeled and deformed. From our point of view, in this review, the most interesting ones are the endoplasmic reticulum (ER) and the Golgi apparatus. The ER is often described as consisting of two different parts: the rough ER and the smooth ER. The rough part consists of flat sacs covered with ribosomes, whereas the smooth part consists of a network of interconnected membrane tubes. These tubes give the ER its characteristic appearance of a net-like labyrinth, which colocalizes with the MT cytoskeleton (see Fig. 7.2, [12, 13]).

In the smooth ER, new tubes are continuously being formed and existing ones disappear [14] by the action of motor proteins that move along MTs [15]. The importance of motors and the cytoskeleton is demonstrated by experiments in which the expression of kinesin is suppressed [16] or the MTs are depolymerized [17]. In both cases the tubular membrane network retracts towards the cell center and no tubes are being formed anymore. Tubular networks can also be observed in cell extracts, providing more insight into the relevant processes involved [18–20]. Such experiments have recently allowed for the determination of the forces required to form tubes from Golgi and ER membranes [21].

The Golgi apparatus is often characterized as a stack of flattened membrane sacs. Like the ER, the Golgi apparatus is also a dynamic organelle. On the cis side membranous cargo carriers that arrive from the ER fuse with the Golgi membrane, while on the trans side tubulovesicular membrane compartments form [22] and pinch off for further transport [23]. Motor proteins that move along MTs have been suggested to form and extend these tubes.

In addition to the shaping of larger organelles, motor proteins and the cytoskeleton are essential for intracellular transport as well. The compartmen-

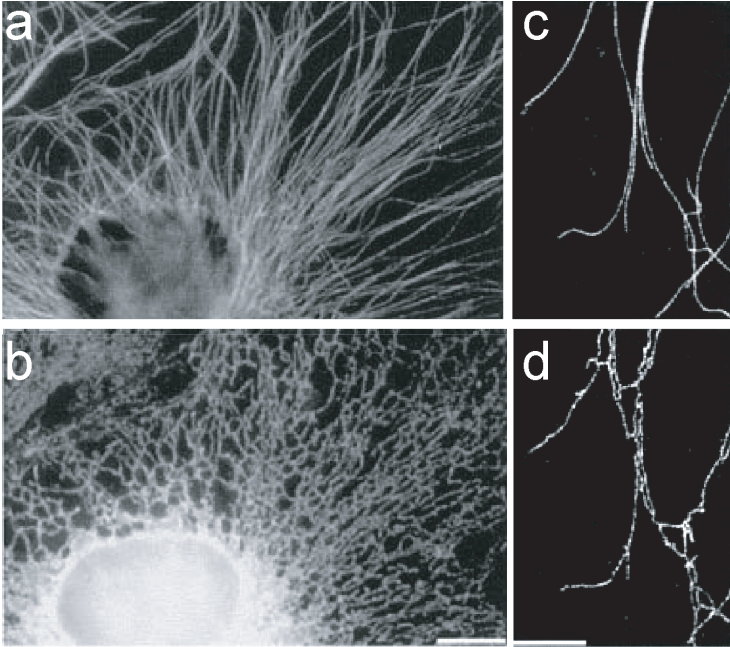


**Fig. 7.2.** Fluorescently labeled microtubules (a) and endoplasmic reticulum (b) are distributed in vivo throughout the cell, and show a close colocalization (c and d). Adapted from [12]. The bar in (b) is 10  $\mu\text{m}$  and in (d) is 5  $\mu\text{m}$

talization of the cell requires the movement of material between the different organelles. Cargo carriers for intracellular transport are small membrane compartments. Historically, it was thought that they had a spherical shape, and were around 100 nm in size. Recent advances in microscopy, especially the specific fluorescent labeling of proteins (GFP technology [24]) have led to the observation that transport carriers in fact have many different shapes. For example, large parts of tubes formed from the Golgi apparatus are cleaved off at once, and subsequently transported [23, 25]. This process of cleavage, the correct movement to the target organelle and the subsequent fusion are intricate processes themselves that require the activity and assembly of protein complexes and cofactors on the membrane [26, 27].

Motor proteins are not the only molecules that can generate localized forces and pull out tubes from membranes. When polymerizing cytoskeletal filaments hit a flat membrane, then they can also generate tubes by pushing the membrane further. Polymerization forces can potentially even be larger ( $\sim 50$  pN for MTs [28]) than the maximal force that a single motor protein can exert. Cilia and flagella [29] are such MT-based protrusions of the plasma membrane (cell membrane). They are responsible for the movement of a variety of eukaryotic cells. In addition, filopodia [29], which are exploratory motile

structures that form and retract with great speed, are generated by rapid local growth of actin filaments that push out the plasma membrane. Adhesive fingers between cells can also be formed by actin polymerization [30]. Recent experiments show that intercellular nanotube networks can be generated via actin polymerization (in rat neural and kidney cells [31], and also in human immune cells [32]) or via transient cell-cell contact (in human immune cells [33]), and that these networks provide a novel mechanism for intercellular communication.

Even though the important role of motor proteins and the cytoskeleton for membrane tube formation is well-established, it should be noted that there are other mechanisms through which curvature may be imposed on membranes that result in shape changes. One may for example think of the assembly of a protein coat with an intrinsic curvature on the membrane, or proteins or lipids that change the local composition of one of the monolayers [34, 35].

### 7.1.2 In Vitro Experiments

For a better understanding of the relevant physics involved in tube formation and to measure the elastic properties of membranes, several experimental techniques have been developed for pulling nanotubes from cell membranes and synthetic vesicles. Historically, membrane nanotubes (tethers) were first observed to be formed from red blood cells attached to glass surfaces and subjected to hydrodynamic flows [36]. This was later followed by other hydrodynamic flow experiments [37, 38], and the application of small beads that are attached to the membranes and manipulated mechanically [39–41] or via optical and magnetic tweezers [21, 42–48]. Very recently, motor proteins and polymerizing MTs have been used to form membrane tubes from artificial vesicles [47, 49–51]. Sheetz and co-workers have also shown that tubes can be extracted from neuronal growth cones and other cells with optical tweezers and were able to measure the extrusion force as a function of length [52–54]. In all cases, tethers were shown to be mainly membranous, i.e., devoid of cytoskeleton [55, 56].

In addition to the studies of individual nanotubes, networks of tubes between membrane vesicles have also been built for biotechnological applications [57–61]. Fluid in such tubes can be transported via surface tension difference: Marangoni flow drives the membrane and hence the fluid inside the connecting tubes towards vesicles of higher tension, while Poiseuille flow (induced by Laplace pressure) occurs in the opposite direction [58, 62]. For giant vesicles the Marangoni flow dominates. When more than one tubes is pulled from the same vesicle, then they tend to attract each other and coalesce [63]. Such coalescence has been observed experimentally [57, 61] and also used to measure the elastic properties of membranes [64].

## 7.2 Theory of Membrane Tubes

The basic question concerning membrane tubes is: why they form in the first place. When a largely flat piece of membrane is grabbed at a point (by a bead, motor protein, or a cytoskeletal filament) and pulled away, one would naturally expect the formation of some cone-like object rather than a narrow tube. An illustrative answer is that because membranes are usually under tension, they try to reduce their surface. The minimum surface area configuration is reached when the membrane is retracted to its original flat conformation and becomes connected to the point of pulling by an infinitesimally narrow tether (having practically zero surface area). As the membrane shrinks towards this tether, however, its curvature increases. And because membranes do not favor large curvatures, the bending rigidity will eventually prevent the membrane from collapsing entirely into such an infinitesimally narrow tether. The result is a narrow tube, the radius of which is set by the balance between the surface tension and the bending rigidity.

### 7.2.1 Free Energy of Membranes

To calculate the radius of membrane tubes and also to study tube formation, let us turn to the elastic theory of two-dimensional liquid bilayers. A general theoretical framework has been developed for the last three decades [65, 66]. In the earliest description [67, 68], known as the spontaneous curvature (SC) model, the membrane is treated as a thin sheet and locally characterized by its mean curvature

$$H = \frac{1}{2} \left( \frac{1}{R_1} + \frac{1}{R_2} \right), \quad (7.1)$$

where  $R_1$  and  $R_2$  are the two principal radii of curvature, as illustrated in Fig. 7.3a. The energy of the membrane, the so-called Helfrich-Canham free energy, is defined as

$$\mathcal{F}_{\text{H-C}} = \int \left[ \frac{\kappa}{2} (2H)^2 - \kappa 2HC_0 \right] dA, \quad (7.2)$$

where  $\kappa$  denotes the bending rigidity of the membrane,  $C_0$  is the spontaneous curvature (characterizing the asymmetry of the membrane if either the lipid composition or the surrounding medium is different on the two sides), and the integral goes over the entire surface of the membrane. The equilibrium shape of the membrane can then be found by minimizing this free energy while obeying system-specific constraints and boundary conditions.

In case of vesicles, e.g., the surface area  $A$  and the enclosed volume  $V$  are often considered constants ( $A_0$  and  $V_0$ , respectively). These constraints can be taken into account by complementing the free energy with the terms  $\sigma A - pV$ , where  $\sigma$  and  $p$  are Lagrange multipliers. If, in addition to this, the distance  $L$  between the two poles of the vesicle along the  $z$  direction are also

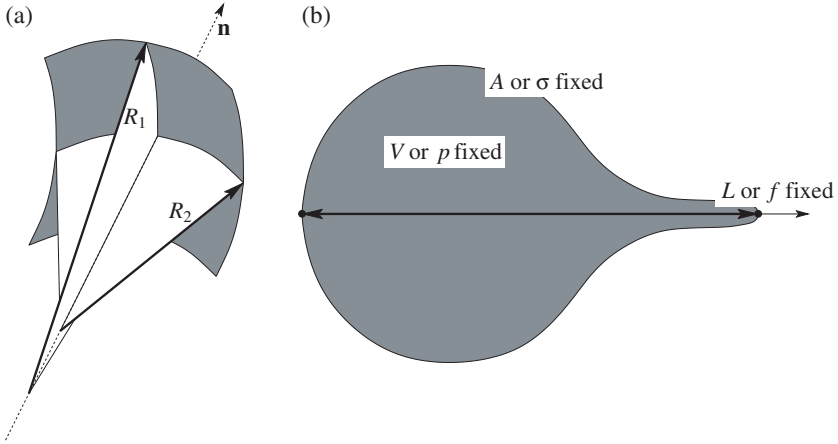


**Fig. 7.3.** (a) Sketch of a piece of membrane, with the two principal radii of curvature ( $R_1$  and  $R_2$ ) and the normal vector of the surface ( $\mathbf{n}$ ) indicated. (b) Either the extensive variables (such as  $A$ ,  $V$ , and  $L$ ) or their intensive conjugate variables ( $\sigma$ ,  $p$ , and  $f$ ) are kept fixed during the minimization of the free energy of the membrane

kept fixed ( $L_0$ ), then the term  $-fL$  should also be added to the free energy, where  $f$  is again a Lagrange multiplier (for illustration see Fig. 7.3b). Thus, the function to be minimized becomes:

$$\mathcal{F} = \mathcal{F}_{\text{H-C}} + \sigma A - pV - fL . \quad (7.3)$$

The values of these Lagrange multipliers will have to be chosen such that the corresponding constraints ( $A = A_0$ ,  $V = V_0$ , and  $L = L_0$ ) be fulfilled. Then the physical meaning of  $\sigma$ ,  $p$ , and  $f$  will become the surface tension of the membrane, the pressure difference between the inside and the outside of the vesicle, and the pulling force at the poles, respectively. This can be easily demonstrated through, e.g., the pulling force: at the minimum of  $\mathcal{F}$ , any of its first derivatives must be zero, thus, for fixed values of  $A$  and  $V$  the derivative  $\partial\mathcal{F}/\partial L = \partial\mathcal{F}_{\text{H-C}}/\partial L - f$  (representing an infinitesimal length change) is also zero, i.e.,  $-f = -\partial\mathcal{F}_{\text{H-C}}/\partial L$ , which is indeed, by definition, the force exerted by the membrane (or conversely,  $f$  is the external force pulling on the membrane).

Here we note that a term proportional to the integral of the Gaussian curvature (which is also quadratic in the curvature, because it is the product of the two principal curvatures) could also be included in the Helfrich-Canham free energy. But since such an integral is a topological invariant, it can be ignored in the energy minimization for vesicles.

If the surface area of the membrane is not constant, either because it is in contact with a lipid reservoir at a fixed chemical potential (as is often the case for biological membranes [44]), or because we are interested in only a small part of the vesicle (as in case of tube formation), then the constraint  $A = A_0$

is released, the rest of the world at the boundaries of the membrane can be replaced by a surface tension  $\sigma$  and, thus, the term  $\sigma A$  will become a real free energy contribution. Similarly, if instead of volume and length constraints, the conjugate variables (i.e., the pressure difference  $p$  and the pulling force  $f$ ) are controlled, then the  $-pV$  and  $-fL$  terms will also become real contributions to the free energy (for illustration see also Fig. 7.3b).

Since a membrane is a bilayer (consisting of two monolayers of lipids), the description of a thin sheet is not always adequate. An additional term needs to be incorporated that takes into account the coupling between the two monolayers. When a bilayer is bent, the outer layer is stretched, while the inner monolayer is compressed. This differential stretching is the essence of the area difference elasticity (ADE) model [69], also known as the generalized bilayer-couple model [70] and it contributes an additional term (quadratic in the deviation of the area difference between the two layers  $\Delta A$  from the preferred value  $\Delta A_0$ ) to the free energy. Although not all experimentally observed shapes and shape transitions can be explained by this model, for most cases the predicted behavior agrees well with the observations [71].

Since for short membrane tubes the free energy contribution of the differential stretching is much smaller than the other terms [72], we will omit it in the rest of this chapter. Similarly, in case of nanotubes the pressure term is also negligible [63, 70, 72, 73], and will be omitted. Thus, for the description of membrane tubes we will consider the following free energy:

$$\mathcal{F} = \int \left[ \frac{\kappa}{2} (2H)^2 - \kappa 2HC_0 + \sigma \right] dA - fL. \quad (7.4)$$

### 7.2.2 Effects of Membrane Proteins and Lipid Composition

So far we have considered the membranes to be spatially homogeneous. While this is indeed the case in most experiments with artificial vesicles, real biological membranes are usually made up of various different kinds of lipids and they also contain membrane proteins. If the different lipids and proteins have different elastic properties (e.g., contribute differently to membrane rigidity) then, as their distributions couple to the local membrane geometry, they can become inhomogeneously distributed or even cause shape instabilities (budding, pearling, fission, etc.) [74–80]. On top of this, the different molecular species, due to the different interactions between them, can even phase separate into distinct domains [81–83]. Such inhomogeneities and domain formations have often been observed experimentally (for examples in relation to membrane tubes see [35, 84–87]), and might be highly relevant in biological processes (such as protein and lipid sorting, or vesiculation).

As the simplest case, let us consider a two-component membrane and expand the free energy contribution of its local composition upto quadratic order in the mean curvature of the membrane ( $2H$ ) and the concentration  $\Phi$  of one of the two constituents:



$$\mathcal{F}_{\text{comp}} = \int \left[ -\lambda 2H\Phi - \mu\Phi + \frac{\chi}{2}\Phi^2 \right] dA, \quad (7.5)$$

where  $\lambda$  is the coupling constant between the curvature and the concentration,  $\mu$  can be regarded as a chemical potential, and  $\chi$  as a susceptibility coefficient [74–76, 88]. The first experimental measurements of these parameters in case of a transmembrane protein have been reported very recently in [89].

Now the total free energy, which is the sum of Eqs. (7.4) and (7.5), has to be minimized with respect to both the geometry of the membrane and the concentration distribution  $\Phi$ . However, since only  $\mathcal{F}_{\text{comp}}$  depends on  $\Phi$ , and only in a quadratic fashion, it alone can be minimized very easily with respect to  $\Phi$ . The obtained minimum can then be added to Eq. (7.4) to get the effective total free energy, which thus depends only on the membrane geometry. It turns out that this effective free energy has the same functional form as Eq. (7.4), in other words, the presence of a second molecular species in the membrane simply rescales the elastic parameters of the membrane [90]. Therefore, in the following we will restrict ourself to the free energy as defined in Eq. (7.4).

### 7.2.3 Formation of Membrane Tubes

The radius of a long tube can easily be derived from Eq. (7.4). For a cylinder of radius  $R$  (yielding  $2H = 1/R$ ) and length  $L$  the free energy simplifies to:

$$\mathcal{F} = \left( \frac{\kappa}{2} \frac{1}{R} - \kappa C_0 + \sigma R \right) 2\pi L - fL. \quad (7.6)$$

Minimizing this with respect to  $R$  results in

$$R_0 = \sqrt{\frac{\kappa}{2\sigma}} \quad (7.7)$$

for the tube radius. Plugging this back into Eq. (7.6), the free energy can be written as

$$\mathcal{F} = 2\pi\kappa \left( \frac{1}{R_0} - C_0 \right) L - fL. \quad (7.8)$$

Since this function is linear in  $L$ , the tube force  $f_0$  (i.e., the force necessary to hold the tube) can be calculated by taking this free energy equal to zero:

$$f_0 = 2\pi\kappa \left( \frac{1}{R_0} - C_0 \right). \quad (7.9)$$

If a pulling force  $f$  larger than  $f_0$  is applied, then the free energy becomes negative and the tube grows to infinity, whereas if  $f$  is smaller than  $f_0$ , then the free energy is positive and, therefore, the tube retracts.

Note, that the tube force  $f_0$  vanishes at  $C_0 = 1/R_0$ . For even larger spontaneous curvatures the tube force becomes negative, signaling that the membrane is unstable, and tubes will grow spontaneously even without pulling.

Interestingly, the tubes themselves will also become unstable against pearling above this critical spontaneous curvatures [72,90,91], thus, the growing objects will look like necklaces rather than tubes [86].

Although the calculation of the tube radius  $R_0$  and tube force  $f_0$  has been an easy exercise, the initial formation of the tubes is a non-trivial process. For  $C_0 = 0$  the force starts to increase linearly as the flat membrane gets deformed, and then reaches a maximum (which is about 13% higher than  $f_0$ ) before it converges to  $f_0$  with an exponentially damped oscillation [63, 70, 73, 92], see Fig. 7.4. For larger  $C_0$ , but still below  $1/R_0$  (an illustration for  $C_0 = 0.9/R_0$  can also be seen in Fig. 7.4) the oscillations of the force become much more pronounced, pearls appear initially, and even the long and well developed tubes get connected to the flat part of the membrane by extremely narrow necks, which can be prone to fission [90]. Thus, the curvature sensitivity of membrane proteins and the pulling of motor proteins together can easily lead to vesiculation.

The shapes and forces just described and exhibited in Fig. 7.4 have been calculated by numerically solving the so-called shape equations (for more details see [63]), which can be derived from the free energy of the membrane by variational methods [93–96].

In most experiments with artificial vesicles the spontaneous curvature can be considered zero. In this case the tube force simplifies to  $f_0 = 2\pi\sqrt{2\sigma\kappa}$ . This theoretical prediction has been verified experimentally [41,45,97,98], and also used for determining the bending rigidity  $\kappa$  of membranes.

For biological membranes the value of  $\kappa$  is usually in the  $10^{-20} - 10^{-19}$  J range and the surface tension  $\sigma$  varies between  $10^{-3}$  and  $10^{-6}$  N/m [65]. Choosing some typical values ( $\kappa \approx 4 \times 10^{-20}$  J and  $\sigma \approx 5 \times 10^{-5}$  N/m) and ignoring the spontaneous curvature one finds that  $R_0 \approx 20$  nm and  $f_0 \approx 12.6$  pN. Thus, in agreement with the multitude of experimental observations, membrane nanotubes are indeed a few tens of nanometers wide, and can be formed by forces around ten piconewtons, which can be easily generated by either the pushing of polymerizing filaments or the pulling of a couple of motor proteins.

Because at the tip of the tubes the mean curvature (and thus the free energy density) of the membrane diverges [63,92,99], for biological systems it seems reasonable to protect the tips and distribute the pulling forces at larger areas (e.g., by utilizing cap proteins or lipid rafts). Recent in vitro experiments have demonstrated that if the pulling area greatly exceeds the tube radius, then a significant force barrier has to be overcome during tube formation, which depends linearly on the radius of the pulling area [46,48,100]. This observation is in good agreement with theoretical predictions [48].

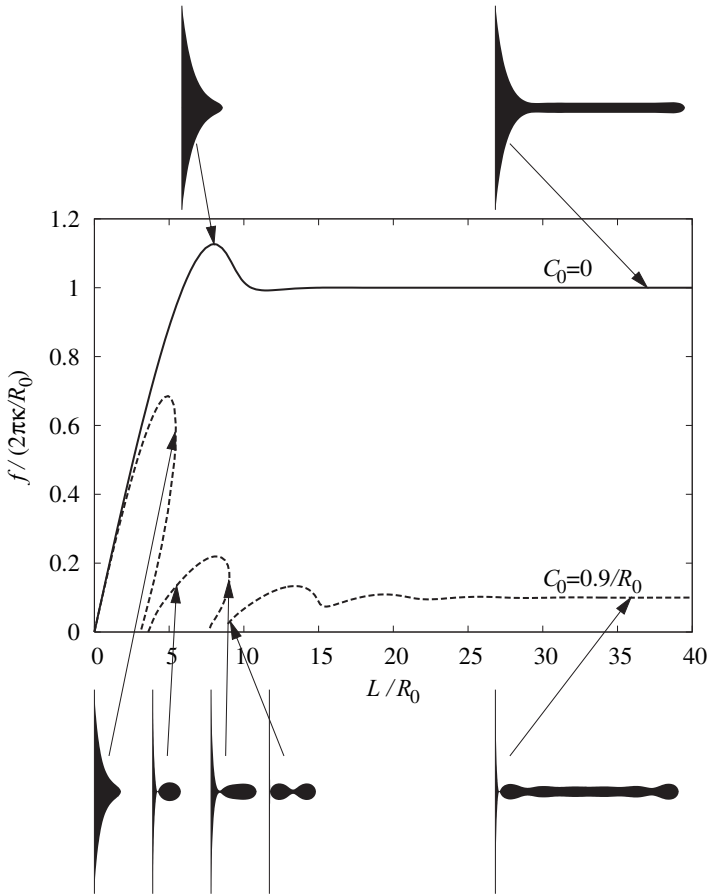


**Fig. 7.4.** Force vs. length curves for the formation of a membrane tube pulled out of a flat membrane that spans a ring of radius  $20R_0$  for two different values of the spontaneous curvature ( $C_0 = 0$  and  $C_0 = 0.9/R_0$ ). The shape of the emerging tube is also depicted at certain stages

### 7.3 Membrane Tube Formation by Cytoskeletal Motor Proteins

The properties of individual motor proteins are being unraveled at a rapid pace. Much less is known about how and whether multiple motors *cooperate*, *interact*, and *coordinate* their activities. Although individual motors could in principle move objects (such as vesicles, DNA, proteins, membrane tubes, etc.), *in vivo* they often function together in groups. Many organelles are observed to move over larger distances than one motor can move [101], suggesting that multiple motors are working together. Cooperative functioning is also thought to be important for the spatial distribution and

morphology of organelles: multiple motors of opposite directionality are present on organelles [102, 103], and it is yet unclear how their interaction is orchestrated [104, 105]. Here, we will discuss recent *in vitro* studies that shed some light on how motor proteins cooperate to generate enough force to form and maintain membrane tubes. Next, we will discuss some promising future studies to tackle the problem of oppositely directed motors, and we will give some first results.

### 7.3.1 *In vitro* Studies Demonstrate that Molecular Motors Cooperatively Pull Membrane Tubes

Recent *in vitro* experiments with purified motors and synthetic vesicles have shed some light on the cooperative activity of motor proteins. When purified motors were linked to beads, which were subsequently attached to a giant unilamellar vesicle (GUV), and then these bead-motor-complex coated vesicles were brought into contact with a network of MTs, the formation of membrane tubes was observed (see Fig. 7.5a [49]). The fact that the force required to form a tube is usually higher than what a single motor protein can exert suggests that each bead was pulled by several motors simultaneously. In contrast, in other experiments with no beads (see Fig. 7.5b [51, 106]), it was found that motors do not need to be cross-linked into multi-motor complexes for tube formation. It was demonstrated that the extent of tube formation depends on the concentration of motor proteins on the vesicle and the force that is required to form a tube (set by global parameters like the membrane tension and the bending rigidity). This led to the proposed mechanism of dynamic association of motor proteins [51]: a steady-state cluster of motor proteins is dynamically maintained at the tip of a membrane tube, taking into account a force dependent departure rate of motor proteins [107, 108] and a concentration dependent arrival rate into the cluster. By simultaneously fluorescent and biotin labeling of lipids, Leduc and Campàs et al. [50] succeeded in the experimental demonstration of clusters at the tip of a tube. Their accompanying theoretical description, which takes into account on and off rates of motors and the active flux of motors along the tube as well, allowed for the quantitative determination of parameters like the motor binding rate and the minimal number of motors required for the extraction of a tube.

All the above-mentioned *in vitro* experiments were conducted with a biotinylated kinesin motor [109], which is a processive dimer. To determine whether tube formation by dynamic clusters of motor proteins is a robust and general mechanism, we recently studied the tube-formation potential of a biotinylated *ncd* motor. This motor was attached to GUVs, and interestingly, after getting into contact with a network of MTs, the first results indicate that *ncd* motors are also able to pull membrane tubes [110]. This process seems to occur in a similar manner as tube formation by kinesin. Some differences are that tube formation occurs at a low velocity (in agreement with the velocity of *ncd*-mediated bead movement [10]) and a higher concentration of *ncd*

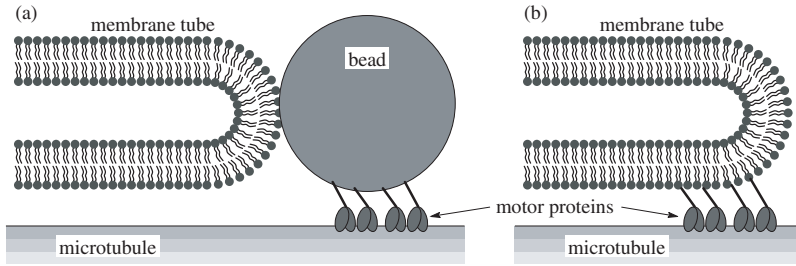


**Fig. 7.5.** Sketches of the *in vitro* experiments, where membrane nanotubes are formed by biotinylated motor proteins that pull on biotinylated lipids either (a) indirectly with the help of streptavidin coated vesicles or (b) directly through individual streptavidin molecules

is required for the same tube-formation potential as kinesin. As individual *ncd* motors are not processive, this result reveals an interesting cooperativity-effect: even if individual motors are non-processive, their joined activity can result in long-distance (processive) movement and drive tube formation and extension under an opposing load.

Interestingly, a recent finding indicates that the binding of motors is enhanced close to where other motors are bound [111]. This could stimulate the (dynamic) formation and stabilization of clusters of motors, which in turn would facilitate long distance movement and tube formation.

### 7.3.2 Interaction between Clusters of Antagonistic Motors?

There is substantial evidence that oppositely directed (antagonistic) motors are simultaneously attached to membrane organelles in the cell. This leads to bi-directional movement of organelles [102–105], and the morphology of membrane structures may also be dependent on such antagonistic motors [102]. In addition to a sufficiently high force, for membrane tube formation another requirement is that a sufficiently high counterforce is exerted on a membrane vesicle, as in the absence of a counterforce the vesicle would be dragged along. This counterforce may be generated by static linkers that immobilize a membrane vesicle, or can be developed by motors that exert force in the opposite direction.

To study the interaction between antagonistic clusters of motors, (plus-end directed) kinesin and (minus-end directed) *ncd* were simultaneously attached to the same vesicle. These motor-coated vesicles were brought into contact with a diluted concentration of immobilized MTs (in order to have only one MT as an interaction partner). Subsequently, a vesicle was grabbed with optical tweezers, and placed on top of the MT. In Fig. 7.6 we present a first result of such an experiment. After placing the vesicle on top of a MT, it started moving. This movement continued for several tens of micrometers,

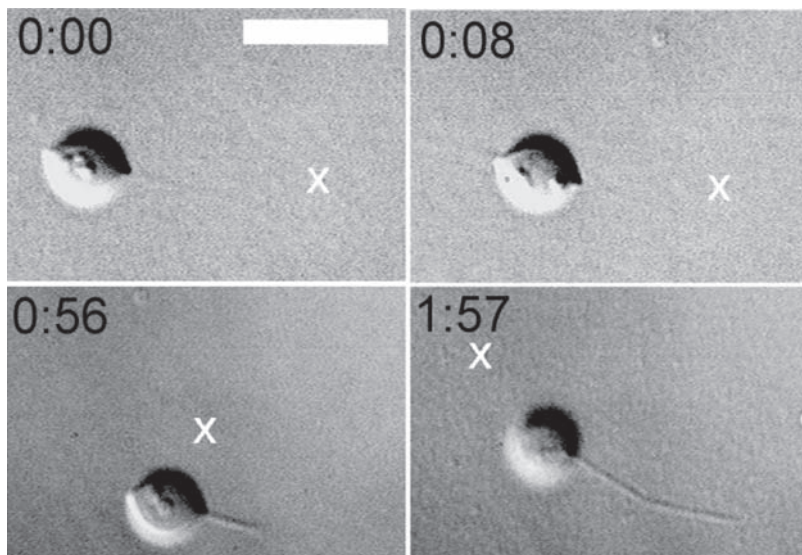


**Fig. 7.6.** VE-DIC microscopy of a membrane tube formed from a vesicle coated with kinesin and ncd. Microtubules are hardly visible. The mark X indicates a reference point on the surface of the coverglass. Time is in minutes and seconds. The bar is 10  $\mu\text{m}$

after which it stopped, while (at the same time) a membrane tube was formed and extended along the MT at about 0.4 micron/second.

Clearly more experiments are required, but one intriguing interpretation of this result is the following: first, the vesicle is moved along a MT by a cluster of motors (presumably kinesin, since it moves at  $\sim 0.4 \mu\text{m/s}$ ), Next, a cluster of ncd motors is nucleated at the trailing end of the vesicle, supplying sufficient counterforce to stop the movement of the vesicle by kinesin. Finally, as the cluster of kinesin motors can generate a high enough force the tug-of-war results in the formation of a tube.

An interesting point here is that naively one would expect two tubes to be formed, since motors are pulling in two opposing directions. It is, however, not energetically favorable to form two tubes, since in this case two neck regions with a high curvature need to be created [70], making it more favorable to extend an already existing tube. Also, the force (energy) barrier required to form a tube is larger than the force required to extend an existing tube [63,73], depending on the size of the area on which the force is exerted [48]. Thus, two tubes will only be formed if the vesicle is held at its position by an additional force.

Our preliminary data suggest that the competition between antagonistic clusters of motor proteins can lead to membrane tube formation. This tube formation is an additional degree of freedom, and it would prevent a tug-of-war in which case neither group of motors can move. Interestingly, the tubes

effectively function as a sorting tool, since only motor proteins that move in one direction will move into and be enriched on a tube. If the tube were subsequently pinched off from the main vesicle body, the plus- and minus-end directed motors and their attached cargo would be segregated.

One important note is that, in the experiments where just kinesin is present on the vesicles and tubes are formed, kinesin motors supply the counterforce that holds the GUV by moving in all directions on the high-density network of randomly oriented MTs. It cannot be excluded that the interaction of the vesicle with the surface, or the presence of rigor motors may also play a role in the immobilization of the vesicle. In order to have interpretable experiments, in the antagonistic motor assay, the density of MTs on the surface was diluted to prevent the interaction of motor-coated vesicles with multiple MTs. However, this method does not prevent the interaction of the vesicle with the coverslip's surface. For a proper study of the interactions between antagonistic motor proteins, it will be important to immobilize the MTs, and at the same time prevent the vesicles from adhering. This is a big challenge since the underlying reason that MTs attach to a surface (charge), also makes the vesicles attach. A possible work-around for this issue is to use vesicles of a different charge. Alternatively, an elegant method may be to construct 3D structures like pillars [112] where MTs reach from one side to the other, and the middle part is not in contact with any surface. Vesicles can then be brought into contact with the elevated MT using the tweezers.

A subject connected with the antagonistic motors is the bi-directional movement of organelles that is observed in cells. When oppositely directed motors are present on a smaller vesicle, instead of tube formation their activity may lead to bi-directional movement (as tube formation from smaller vesicles will require a higher force because there is less excess surface area). Generally it is suggested that “coordination machinery” exists that controls whether one kind of motor or the other is active [104, 105], however, the physical interaction of antagonistic clusters of motors (transmitted through the vesicle) might play a role as well. One can imagine that at low motor concentrations, stochastic fluctuations in the number of motors may lead to alternating stable clusters of plus-end or minus-end directed motors, in turn leading to bi-directional movement. In that case the dynamical transition of collections of motors would act as number fluctuation amplifier [113–115]. The details of such “metastable” bi-directionality should depend on the rate of arrival into and the rate of departure from a cluster of motors [51, 110]. A further discussion of this bi-directionality is outside the scope of this work, but experiments are on the way to determine this system in more detail, and establish the regulatory role of physical parameters on antagonistic clusters of motors.

It is now well established that force-generating motor proteins are sufficient and enough for membrane tube formation. Resolving how (physical) parameters may regulate the dynamic interplay between motors and membranes is a promising line of research.

## Acknowledgments

I. D. acknowledges support from the Hungarian Science Foundation (Grant No. OTKA F043756). The contribution by G. K. and M. D. is part of the research program of the “Stichting voor Fundamenteel Onderzoek der Materie (FOM)”, which is financially supported by the “Nederlandse organisatie voor Wetenschappelijk Onderzoek (NWO)”.

## References

1. K. Visscher, M. J. Schnitzer, S. M. Block (1999). *Nature*, **400**, pp. 184–189
2. J. Howard. *Mechanics of motor proteins and the cytoskeleton*, (Sinauer Associates, Sunderland 2001)
3. K. Svoboda, C. F. Schmidt, B. J. Schnapp, S. M. Block (1993). *Nature*, **365**, pp. 721–727
4. H. B. McDonald, L. S. B. Goldstein (1990). *Cell*, **61**, pp. 991–1000
5. W. Hua, J. Chung, J. Gelles (2002). *Science*, **295**, pp. 844–848
6. C. L. Asbury, A. N. Fehr, S. M. Block (2003). *Science*, **302**, pp. 2130–2134
7. R. D. Vale (2003). *J. Cell Biol.*, **163**, pp. 445–450
8. A. Yildiz, M. Tomishige, R. D. Vale, P. R. Selvin (2004). *Science*, **303**, pp. 676–678
9. R. D. Vale (2003). *Cell*, **112**, pp. 467–480
10. M. W. Allersma, F. Gittes, M. J. deCastro, R. J. Stewart, C. F. Schmidt (1998). *Biophys. J.*, **74**, pp. 1074–1085
11. R. Chandra, E. D. Salmon, H. P. Erickson, A. Lockhart, S. A. Endow (1993). *J. Biol. Chem.*, **268**, pp. 9005–9013
12. J. Lane, V. Allan (1999). *Mol. Biol. Cell*, **10**, pp. 1909–1922
13. M. Terasaki, L. B. Chen, K. Fujiwara (1986). *J. Cell Biol.*, **103**, pp. 1557–1568
14. C. Lee, L. B. Chen (1988). *Cell*, **54**, pp. 37–46
15. C. M. Waterman-Storer, E. D. Salmon (1998). *Curr. Biol.*, **8**, pp. 798–806
16. F. Feiguin, A. Ferreira, K. S. Kosik, A. Caceres (1994). *J. Cell Biol.*, **127**, pp. 1021–1039
17. C. H. Lee, M. Ferguson, L. B. Chen (1989). *J. Cell Biol.*, **109**, pp. 2045–2055
18. S. L. Dabora, M. P. Sheetz (1988). *Cell*, **54**, pp. 27–35
19. R. D. Vale, H. Hotani (1988). *J. Cell Biol.*, **107**, pp. 2233–2241
20. V. Allan, R. D. Vale (1994). *J. Cell Sci.*, **107**, pp. 1885–1897
21. A. Upadhyaya, M. P. Sheetz (2004). *Biophys. J.*, **86**, pp. 2923–2928
22. H. H. Mollenhauer, D. J. Morré (1998). *Histochem. Cell Biol.*, **109**, pp. 533–543
23. N. Sciaky, J. Presley, C. Smith, K. J. M. Zaal, N. Cole, J. E. Moreira, M. Terasaki, E. Siggia, J. Lippincott-Schwartz (1997). *J. Cell Biol.*, **139**, pp. 1137–1155
24. J. Lippincott-Schwartz, E. Snapp, A. Kenworthy (2001). *Nat. Rev. Mol. Cell Biol.*, **2**, pp. 444–456
25. E. V. Polishchuk, A. Di Pentima, A. Luini, R. S. Polishchuk (2003). *Mol. Biol. Cell*, **14**, pp. 4470–4485
26. T. Kirchhausen (2000). *Nat. Rev. Mol. Cell Biol.*, **1**, pp. 187–198
27. J. S. Bonifacino, B. S. Glick (2004). *Cell*, **116**, pp. 153–166



28. M. Dogterom, J. W. J. Kerssemakers, G. Romet-Lemonne, M. E. Janson (2005). *Curr. Opin. Cell Biol.*, **17**, pp. 67–74
29. B. Alberts, A. Johnson, J. Lewis, M. Raff, K. Roberts, P. Walter: *Molecular Biology of the Cell*, 4th edn (Garland Science, New York 2002)
30. H. Delanoë-Ayari, P. Lenz, J. Brevier, M. Weidenhaupt, M. Vallade, D. Gulino, J. F. Joanny, D. Riveline (2004). *Phys. Rev. Lett.*, **93**, pp. 108102
31. A. Rustom, R. Saffrich, I. Markovic, P. Walther, H.-H. Gerdes (2004). *Science*, **303**, pp. 1007–1010
32. S. C. Watkins, R. D. Salter (2005). *Immunity*, **23**, pp. 309–318
33. B. Önfelt, S. Nedvetzki, K. Yanagi, D. M. Davis (2004). *J. Immunol.*, **173**, pp. 1511–1513
34. K. N. J. Burger (2000). *Traffic*, **1**, pp. 605–613
35. K. Farsad and P. De Camilli (2003). *Curr. Opin. Cell Biol.*, **15**, pp. 372–381
36. R. M. Hochmuth, N. Mohandas, P. L. Blackshear (1973). *Biophys. J.*, **13**, pp. 747–762
37. R. E. Waugh (1982). *Biophys. J.*, **38**, pp. 29–37
38. O. Rossier, D. Cuvelier, N. Borghi, P. H. Puech, I. Derényi, A. Buguin, P. Nassoy, and F. Brochard-Wyart (2003). *Langmuir*, **19**, pp. 575–584
39. R. M. Hochmuth, H. C. Wiles, E. A. Evans, J. T. McCown (1982). *Biophys. J.*, **39**, pp. 83–89
40. R. E. Waugh, J. Song, S. Svetina, B. Zeks (1992). *Biophys. J.*, **61**, pp. 974–982
41. E. Evans, A. Yeung (1994). *Chem. Phys. Lipids*, **73**, pp. 39–56
42. Z. Li, B. Anvari, M. Takashima, P. Brecht, J. H. Torres, W. E. Brownell (2002). *Biophys. J.*, **82**, pp. 1386–1395
43. T. Roopa, G. V. Shivashankar (2003). *Appl. Phys. Lett.*, **82**, pp. 1631–1633
44. D. Raucher, M. P. Sheetz (1999). *Biophys. J.*, **77**, pp. 1992–2002
45. V. Heinrich, R. E. Waugh (1996). *Ann. Biomed. Eng.*, **24**, pp. 595–605
46. H. Hotani, T. Inaba, F. Nomura, S. Takeda, K. Takiguchi, T. J. Itoh, T. Umeda, A. Ishijima (2003). *Biosystems*, **71**, pp. 93–100
47. D. K. Fygenson, J. F. Marko, A. Libchaber (1997). *Phys. Rev. Lett.*, **79**, pp. 4497–4500
48. G. Koster, A. Cacciuto, I. Derényi, D. Frenkel, M. Dogterom (2005). *Phys. Rev. Lett.*, **94**, pp. 068101
49. A. Roux, G. Cappello, J. Cartaud, J. Prost, B. Goud, P. Bassereau (2002). *Proc. Natl. Acad. Sci. USA*, **99**, pp. 5394–5399
50. C. Leduc, O. Campàs, K. B. Zeldovich, A. Roux, P. Jolimaître, L. Bourel-Bonnet, B. Goud, J.-F. Joanny, P. Bassereau, J. Prost (2004). *Proc. Natl. Acad. Sci. USA*, **101**, pp. 17096–17101
51. G. Koster, M. VanDuijn, B. Hofs, M. Dogterom (2003). *Proc. Natl. Acad. Sci. USA*, **100**, pp. 15583–15588
52. J. Dai, M. P. Sheetz (1995). *Biophys. J.*, **68**, pp. 988–996
53. J. Dai, M. P. Sheetz (1999). *Biophys. J.*, **77**, pp. 3363–3370
54. R. M. Hochmuth, J. Y. Shao, J. Dai, M. P. Sheetz (1996). *Biophys. J.*, **70**, pp. 358–369
55. R. E. Waugh, R. G. Bauserman (1995). *Ann. Biomed. Eng.*, **23**, pp. 308–321
56. M. P. Sheetz (2001). *Nat. Rev. Mol. Cell Biol.*, **2**, pp. 392–396
57. E. Evans, H. Bowman, A. Leung, D. Needham, D. Tirrell (1996). *Science*, **273**, pp. 933–935
58. A. Karlsson, R. Karlsson, M. Karlsson, A.-S. Cans, A. Strömberg, F. Ryttsén, O. Orwar (2001). *Nature*, **409**, pp. 150–152

59. M. Karlsson, K. Sott, M. Davidson, A.-S. Cans, P. Linderholm, D. Chiu, and O. Orwar (2002). *Proc. Natl. Acad. Sci. USA*, **99**, pp. 11573–11578
60. M. Karlsson, M. Davidson, R. Karlsson, A. Karlsson, J. Bergenholtz, Z. Konkoli, A. Jesorka, T. Lobovkina, J. Hurtig, M. Voinova, O. Orwar (2004). *Ann. Rev. Phys. Chem.*, **55**, pp. 613–649
61. T. Lobovkina, P. Dommersnes, J.-F. Joanny, P. Bassereau, M. Karlsson, O. Orwar (2004). *Proc. Natl. Acad. Sci. USA*, **101**, pp. 7949–7953
62. P. G. Dommersnes, O. Orwar, F. Brochard-Wyart, J. F. Joanny (2005). *Europhys Lett.*, **70**, pp. 271–277
63. I. Derényi, F. Jülicher, J. Prost (2002). *Phys. Rev. Lett.*, **88**, pp. 238101
64. D. Cuvelier, I. Derényi, P. Bassereau, P. Nassoy (2005). *Biophys. J.*, **88**, pp. 2714–2726
65. U. Seifert, R. Lipowsky. Morphology of Vesicles. In: *Structure and Dynamics of Membranes*, vol 1A, ed by R. Lipowsky, E. Sackmann (Elsevier Science, Amsterdam 1995) pp. 403–462
66. U. Seifert (1997). *Adv. Phys.*, **46**, pp. 13–137
67. W. Helfrich (1973). *Z. Naturforsch. C*, **28**, pp. 693–703
68. P. B. Canham (1970). *J. Theor. Biol.*, **26**, pp. 61–81
69. L. Miao, U. Seifert, M. Wortis, H. G. Döbereiner (1994). *Phys. Rev. E*, **49**, pp. 5389–5407
70. V. Heinrich, B. Bozic, S. Svetina, B. Zeks (1999). *Biophys. J.*, **76**, pp. 2056–2071
71. H. G. Döbereiner, E. Evans, M. Kraus, U. Seifert, M. Wortis (1997). *Phys. Rev. E*, **55**, pp. 4458–4474
72. D. J. Bukman, J. H. Yao, M. Wortis (1996). *Phys. Rev. E*, **54**, pp. 5463–5468
73. T. R. Powers, G. Huber, R. E. Goldstein (2002). *Phys. Rev. E*, **65**, pp. 041901
74. S. Leibler (1986). *J. Phys.*, **47**, pp. 507–516
75. S. Leibler, D. Andelman (1987). *J. Phys.*, **48**, pp. 2013–2018
76. T. Taniguchi, K. Kawasaki, D. Andelman, T. Kawakatsu (1994). *J. Phys. II*, **4**, pp. 1333–1362
77. M. Seul, D. Andelman (1995). *Science*, **267**, pp. 476–483
78. J. B. Fournier (1996). *Phys. Rev. Lett.*, **76**, pp. 4436–4439
79. S. Komura, H. Shirotori, P. D. Olmsted, D. Andelman (2004). *Europhys. Lett.*, **67**, pp. 321–327
80. C.-M. Chen, P. G. Higgs, F. C. MacKintosh (1997). *Phys. Rev. Lett.*, **79**, pp. 1579–1582
81. F. Jülicher, R. Lipowsky (1996). *Phys. Rev. E*, **53**, pp. 2670–2683
82. T. Kawakatsu, D. Andelman, K. Kawasaki, T. Taniguchi (1993). *J. Phys. II*, **3**, pp. 971–997
83. J.-M. Allain, C. Storm, A. Roux, M. Ben Amar, J.-F. Joanny (2004). *Phys. Rev. Lett.*, **93**, p. 158104
84. V. Kralj-Iglic, A. Iglic, M. Bobrowska-Hagerstrand, H. Hagerstrand (2001). *Colloids Surf. A*, **179**, pp. 57–64
85. I. Tsafrir, D. Sagi, T. Arzi, M.-A. Guedeau-Boudeville, V. Frette, D. Kandel, J. Stavans (2001). *Phys. Rev. Lett.*, **86**, pp. 1138–1141
86. I. Tsafrir, Y. Caspi, M.-A. Guedeau-Boudeville, T. Arzi, J. Stavans (2003). *Phys. Rev. Lett.*, **91**, p. 138102
87. B. J. Peter, H. M. Kent, I. G. Mills, Y. Vallis, P. J. G. Butler, P. R. Evans, H. T. McMahon (2004). *Science*, **303**, pp. 495–499

88. S. Ramaswamy, J. Toner, J. Prost (2000). *Phys. Rev. Lett.*, **84**, pp. 3494–3497
89. P. Girard, J. Prost, P. Bassereau (2005). *Phys. Rev. Lett.*, **94**, pp. 088102
90. I. Derényi, A. Czövek, F. Jülicher, J. Prost: (to be published)
91. H. J. Deuling, W. Helfrich (1977). *Blood Cells*, **3**, pp. 713–720
92. B. Bozic, V. Heinrich, S. Svetina, B. Zeks (2001). *Eur. Phys. J. E*, **6**, pp. 91–98
93. F. Jülicher, U. Seifert (1994). *Phys. Rev. E*, **49**, pp. 4728–4731
94. H. Jian-Guo, O.-Y. Zhong-Can (1993). *Phys. Rev. E*, **47**, pp. 461–467
95. W.-M. Zheng, J. Liu (1993). *Phys. Rev. E*, **48**, pp. 2856–2860
96. B. Bozic, S. Svetina, B. Zeks (1997). *Phys. Rev. E*, **55**, pp. 5834–5842
97. R. E. Waugh, R. M. Hochmuth (1987). *Biophys. J.*, **52**, pp. 391–400
98. L. Bo, R. E. Waugh (1989). *Biophys. J.*, **55**, pp. 509–517
99. R. Podgornik, S. Svetina, B. Zeks (1995). *Phys. Rev. E*, **51**, pp. 544–547
100. T. Inaba, A. Ishijima, M. Honda, F. Nomura, K. Takiguchi, H. Hotani (2005). *J. Mol. Biol.*, **348**, pp. 325–333
101. D. B. Hill, M. J. Plaza, K. Bonin, G. Holzwarth (2004). *Eur. Biophys. J.*, **33**, pp. 623–632
102. V. J. Allan, H. M. Thompson, M. A. McNiven (2002). *Nat. Cell Biol.*, **4**, pp. E236–E242
103. C. Kural, H. Kim, S. Syed, G. Goshima, V. I. Gelfand, P. R. Selvin (2005). *Science*, **308**, pp. 1469–1472
104. S. P. Gross (2004). *Physical Biology*, **1**, pp. 1–11
105. M. A. Welte (2004). *Curr. Biol.*, **14**, pp. 525–537
106. C. Leduc (2005). Système biomimétique d’intermediaires de transport tubulaires: étude quantitative. PhD thesis, Université Paris 7, Paris
107. C. M. Coppin, D. W. Pierce, L. Hsu, R. D. Vale (1997). *Proc. Natl. Acad. Sci. USA*, **94**, pp. 8539–8544
108. A. Parmegianni, F. Jülicher, L. Peliti, J. Prost (2001). *Europhys. Lett.*, **56**, pp. 603–609
109. T. Surrey, M. B. Elowitz, P.-E. Wolf, F. Yang, F. Nedelec, K. Shokat, S. Leibler (1998). *Proc. Natl. Acad. Sci. USA*, **95**, pp. 4293–4298
110. G. Koster (2005). Membrane tube formation by motor proteins. PhD thesis, AMOLF, Amsterdam
111. E. Muto, H. Sakai, K. Kaseda (2005). *J. Cell Biol.*, **168**, pp. 691–696
112. W. Roos, J. Ulmer, S. Grater, T. Surrey, J. P. Spatz (2005). *Nano Lett.*, **5**, pp. 2630–2634
113. F. Jülicher, J. Prost (1995). *Phys. Rev. Lett.*, **75**, pp. 2618–2821
114. D. Riveline, A. Ott, F. Jülicher, A. Winkelmann, O. Cardoso, J. J. Lacapere, S. Magnusdottir, J. L. Viovy, L. Gorre-Talini, J. Prost (1998). *Eur. Biophys. J.*, **27**, pp. 403–408
115. M. Badoual, F. Jülicher, J. Prost (2002). *Proc. Natl. Acad. Sci. USA*, **99**, pp. 6696–6701

